Dynamic Interpolation and Application to Flight Control

Joseph W. Jackson*
Honeywell, Inc., Glendale, Arizona 85308
and
Peter E. Crouch†
Arizona State University, Tempe, Arizona 85287

To simplify the specification of a desired trajectory for some subset of the variables of a dynamic control system, it may be advantageous to designate a set of intercept points that the trajectory is required to pass through. The system controls can then be computed in terms of a spline function to meet these requirements for dynamic interpolation. Optimization of a cost function under continuity constraints can be embedded in the determination of spline coefficients to obtain certain desirable geometric properties of the resulting trajectory.

I. Introduction

FORCING certain dynamic variables of a control system to follow a desired path often in conjunction with an optimization routine poses a difficult problem both in theory and practice. The main motivation of this paper is to simplify the problem by not insisting that the variables follow an exact trajectory, but instead track a path specified only in terms of a set of intercept points and continuity constraints. An advantage of the discretely specified path is that the system controls may be segmented between intercept points, allowing the application of piecewise-continuous polynomials to define the segment control. The method of splines,[1,2] commonly used in computer-aided geometric design (CAGD) to define curves and surfaces, can be applied to join these polynomials in an organized fashion. The use of splines on the controls of a dynamic system so as to guide the system through a set of intercept points will herein be termed "dynamic interpolation."

An example of a system that uses a discretely specified path is an aircraft maneuvering to land at an airport. Here, the intercept points, or "waypoints," for the particular airport approach are entered or prestored in the onboard flight management system (FMS). This device then computes the necessary steering commands the pilot or autopilot must follow to guide the aircraft through the points. Certain tolerances are allowed about the waypoints that the aircraft must fly within. Present technology of flight management computers allows computation of a relatively simple path consisting of straight lines and circular arcs that meet the stated waypoint tolerance and afford acceptable passenger comfort.

Air travel has increased tremendously in the U.S. and abroad. This is putting pressure on the air traffic control (ATC) system to alleviate congestion and improve efficiency. One of the main drawbacks to the present ATC system is that aircraft scheduled for arrival are guided along a straight-line path to the runway, so that aircraft landing frequency is based on minimum distance at which aircraft may be safely spaced along the path. Differentiation between aircraft type [fast/slow, slow takeoff and landing (STOL), etc.] is not made. A straight-line approach is used because of the narrow coverage of the instrument landing system that provides guidance to the pilot and/or the autopilot on the approach segment.

The microwave landing system (MLS) was introduced[3] to improve ATC efficiency. MLS provides precision position information to the pilot, navigation, and guidance system over a wide range of coverage in the terminal area, thus making curved-path and steep-descent approach guidance possible. Integration of an FMS capable of generating curved-path approaches with the guidance capability of MLS forms a system that can advance significantly the ATC capacity and efficiency. The integrated system would provide guidance on a curved path to the runway via specified approach waypoints and also a cockpit display of the path error to the pilot. This paper presents results of dynamic interpolation applied to the aircraft approach problem where aircraft total acceleration is minimized, subject to the constraints that the waypoints are intercepted, the final velocity is specified, and the resulting trajectory has continuous jerk. This latter constraint ensures more physically acceptable control trajectories. The intercept times for the waypoints are assumed known. Incorporation of this optimization into present-day FMS computers to improve total system performance will require MLS guidance capabilities, since dynamic interpolation creates paths even more complicated than simple segments of straight lines and circular arcs.

Several papers have been published that report on the optimization of the four-dimensional (fourth dimension is the specified arrival time) curved-path approach. The most pertinent of these to the approach problem under consideration[4-6] perform a minimization of direct operating costs (DOC) using an energy rate model of aircraft performance for the vertical portion of the flight. DOC is made of two components, that of fuel consumption and of arrival time variance. The latter cost recognizes the penalty imposed on the airline when an aircraft arrives early or late relative to its scheduled arrival. The mission is separated into three phases: climb, cruise, and descent. Each phase is considered separately in the optimization. Horizontal maneuvers are confined to segments of straight lines and circular arcs. Waypoints are specified in terms of position coordinates and constraints on aircraft velocity (V_{min}, V_{nom}, V_{max}). The application of our proposed dynamic interpolation method to the four-dimensional aircraft trajectory problem will allow the generation of aircraft controls that minimize a given cost function, be it aircraft acceleration, fuel consumption, early/late arrival time, etc., while maintaining given constraints, such as waypoint interception, velocity constraints, and path continuity requirements. In addition to the specification of splines for the system controls, the potential advantages of dynamic interpolation over previous work[4-6] are the coupling of horizontal and vertical motion and the integration of the complete mission objective into the optimization problem.

Application of optimal control techniques for tracking "discretely specified" trajectories has been attempted in the robotics area.[7,8] Here, a set of desired intercept points for the

Received Jan. 2, 1990; revision received June 22, 1990; accepted for publication July 25, 1990.

*Staff Engineer, Commercial Flight Systems Group.
†Professor, Center for Systems Science and Engineering.

end effector is specified in Cartesian coordinates and transformed into joint angles. The discrete set of joint angle intercepts is then connected with cubic splines to form the desired joint angle trajectory. The solution of the spline coefficients results from an optimization that minimizes total travel time while constraining robot joint velocity, acceleration, and jerk. The resulting Cartesian path does intercept the original Cartesian intercepts, but those segments in which the designer expected straight-line segments are not always straight, due to the "inscribing error" induced by the Cartesian-to-joint angle transformation. To minimize these errors, extra Cartesian intercepts are added to the original set, while keeping the same number of spline segments that determine the joint angle path. A least-squares fit to the desired points is determined in the process. Dynamic interpolation applied to robotics would attempt to specify the joint controls in terms of splines to achieve results under the given constraints and optimizations.

An important property desirable in dynamic interpolation is affine invariance.[9] That is, if the desired intercept points are translated, rotated, or scaled, the trajectory generated from the transformed set via dynamic interpolation should be the same as that found by transforming the entire original trajectory. To enforce affine invariance, the cost functional used must have specific properties, as will be discussed.

Finally, application of dynamic interpolation may generate trajectories that exhibit undesirable characteristics, akin to the preceding robotics example where straight-line segments were expected but not realized. For the aircraft approach example, the intercept times may be adjusted to achieve a more favorable trajectory, or the velocities at the waypoints specified to

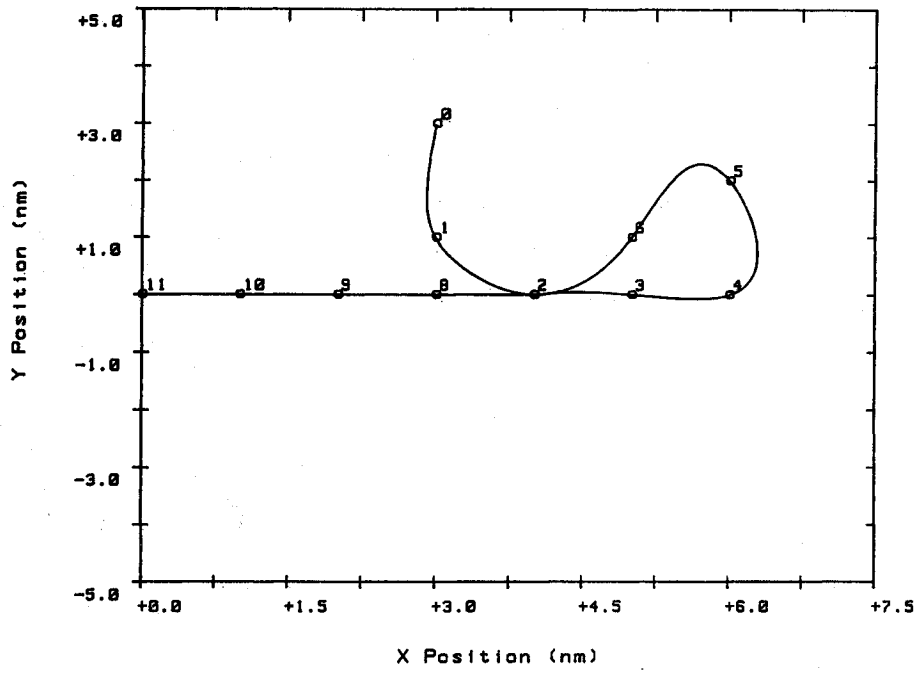

Fig. 1a Static CAGD X vs Y position.

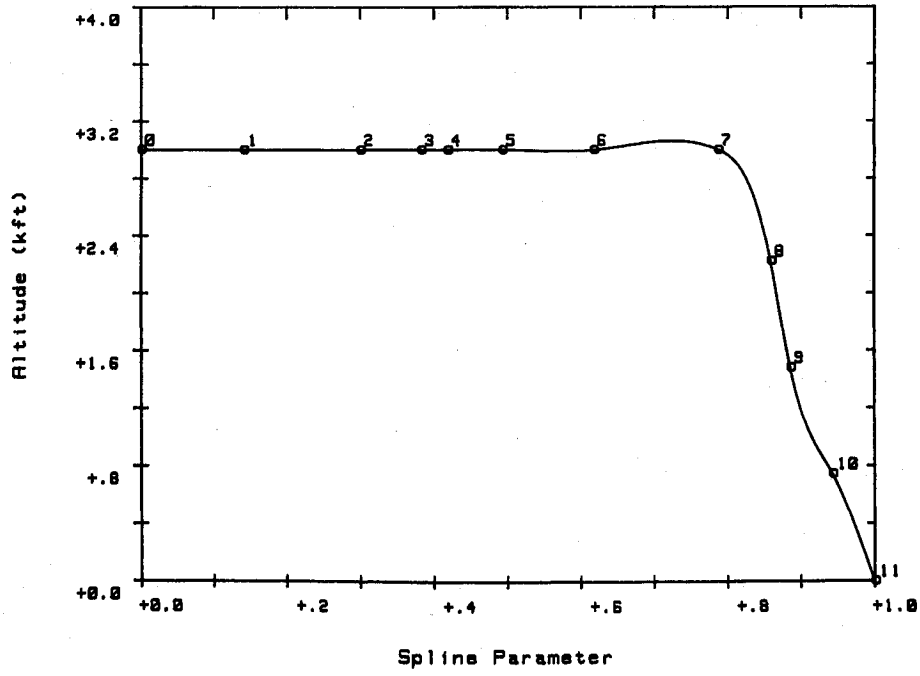

Fig. 1b Static CAGD altitude vs spline parameter.

Table 1 Teardrop approach waypoints

Waypoint	X-axis intercept, nm	Y-axis intercept, nm	H-axis intercept, ft
0	3	3	3000
1	3	1	3000
2	4	0	3000
3	5	0	3000
4	6	0	3000
5	6	2	3000
6	5	1	3000
7	4	0	3000
8	3	0	2222
9	2	0	1481
10	1	0	741
11	0	0	0

Table 2 Intercept times for dynamic trajectory

Interval	Static arclength, ft	Intercept time, s	Dynamic quadratic spline arclength, ft	Dynamic cubic spline arclength, ft
1	12,240	61.2	12,187	12,210
2	9,068	106.5	9,130	9,124
3	6,115	137.1	6,088	6,089
4	6,170	168.0	6,228	6,242
5	13,008	233.0	12,727	12,736
6	11,886	292.4	9,401	9,460
7	9,103	338.0	8,814	8,818
8	6,130	368.6	6,161	6,163
9	6,125	399.2	6,126	6,126
10	6,125	430.0	6,126	6,126
11	6,125	460.5	6,127	6,127

avoid stall or placard speed violations. We will return to this discussion in Sec. IV.

II. Application of Cubic Splines to Flight-Path Generation

For our problem—driving a dynamic system through a discrete set of waypoints using simple splines for the control description—it is desirable to have a reference trajectory to compare quantitatively with the path derived dynamically. Work in CAGD has provided flexible methods of applying cubic splines to a set of intercept points so as to achieve desirable trajectories.[1,9,10]

To illustrate the application of splines to an aircraft problem, a set of intercept points was chosen that describes a difficult "teardrop approach" maneuver to an airport. These waypoints are given in Table 1. Note that the touchdown coordinates are (0, 0, 0).

The "static" trajectory resulting from the application of cubic splines to the waypoints given in Table 1 is shown in Fig. 1. This trajectory fits the waypoints very well in all aspects except the altitude deviation before waypoint 7. This deviation could be reduced by moving waypoint 7 halfway between waypoint 6 and 8 altitudes (2593 ft). However, this excursion is used as a critical test of the performance of our control schemes, as will be discussed in Sec. III.

It is interesting to note the well-known fact that the application of cubic splines will yield a curve $b(t)$ which minimizes

$$\int_{t_0}^{t_N} \|\ddot{b}(t)\|^2 \, dt \tag{1}$$

This property shows that cubic splines approximately minimize curvature, given by the expression

$$K = \frac{\|\dot{b}(t) \wedge \ddot{b}(t)\|}{\|\dot{b}(t)\|^3} \tag{2}$$

if total velocity $\|\dot{b}(t)\|$ is nearly constant ($\wedge$ denotes cross product). This is an important reason for the usefulness of cubic splines. However, this property is also important when the statically generated spline curve is used as the reference trajectory with which to compare the trajectory of a dynamic control system, since minimization of squared acceleration can be viewed in many systems as approximating conservation of energy expended while following a trajectory. In the next section, the cost functional applied to the optimization of controls of a dynamic system will include the squared acceleration term for this reason.

III. Application of Dynamic Interpolation to Flight Control

The linearized equations that describe the aircraft motion in Cartesian coordinates (x,y,h) can be expressed in terms of pseudocontrols (U_x,U_y,U_h) as[11]

$$\left.\begin{aligned} \ddot{x}(t) &= U_x(t) \\ \ddot{y}(t) &= U_y(t) \\ \ddot{h}(t) &= U_h(t) \end{aligned}\right\} \quad t_0 \le t \le t_N \tag{3}$$

The pseudocontrols are themselves nonlinear functions of the actual aircraft controls and parameters (e.g., thrust, bank angle, load factor, airspeed, heading, and flight-path angle).

We wish to determine the controls (U_x,U_y,U_h) in terms of Mth-order splines that minimize the functional

$$J = \int_{t_0}^{t_N} [\ddot{x}(s)^2 + \ddot{y}(s)^2 + \ddot{h}(s)^2] \, ds \tag{4}$$

under the point constraints

$$\left.\begin{aligned} x(t_i) &= x_i \\ y(t_i) &= y_i \\ h(t_i) &= h_i \end{aligned}\right\} \quad 0 \le i \le N \tag{5}$$

and the terminal velocity constraints

$$\dot{x}(t_0) = \dot{x}_0, \qquad \dot{x}(t_N) = \dot{x}_N \tag{6a}$$

$$\dot{y}(t_0) = \dot{y}_0, \qquad \dot{y}(t_N) = \dot{y}_N \tag{6b}$$

$$\dot{h}(t_0) = \dot{h}_0, \qquad \dot{h}(t_N) = \dot{h}_N \tag{6c}$$

Differentiability constraints can be second order

$$\left.\begin{aligned} &\dot{x}(t) \text{ continuous} \\ &\dot{y}(t) \text{ continuous} \\ &\dot{h}(t) \text{ continuous} \end{aligned}\right\} \quad t_0 \le t \le t_N \tag{7a}$$

or third order

$$\left.\begin{aligned} &\ddot{x}(t) \text{ continuous} \\ &\ddot{y}(t) \text{ continuous} \\ &\ddot{h}(t) \text{ continuous} \end{aligned}\right\} \quad t_0 \le t \le t_N \tag{7b}$$

We choose the following monomial spline representation of the pseudocontrols:

$$U_x(t) = \sum_{j=0}^{M} G_{x,i}(j) \, (t - t_{i-1})^j / j! \tag{8a}$$

$$U_y(t) = \sum_{j=0}^{M} G_{y,i}(j) \, (t - t_{i-1})^j / j! \tag{8b}$$

$$U_h(t) = \sum_{j=0}^{M} G_{h,i}(j) \, (t - t_{i-1})^j / j! \tag{8c}$$

$$t_{i-1} \le t \le t_i, \qquad 1 \le i \le N$$

where the vectors $G_{x,i}$, $G_{y,i}$, and $G_{h,i}$ contain the pseudocontrol spline coefficients for the ith interval. As noted in Eqs. (7), either second- or third-order differentiability of $x(t)$, $y(t)$, and $h(t)$ will be considered. The minimum order M of the polynomial controls (U_x,U_y,U_h) that minimize the cost functional in Eq. (4) under the constraints in Eqs. (5-7) depends on the order of the continuity constraint in Eqs. (7). For second-order differentiability, we must choose $M = 2$. This may be justified by the following observations. The zero-order coefficients enable the continuity constraints of controls (U_x,U_y,U_h), and, hence, the second-order differentiability constraints of the states $x(t)$, $y(t)$, and $h(t)$ to be satisfied. The first-order coefficients enable the intercept point constraints to be met. Finally, the second-order coefficients are satisfied by using the optimization procedure. Note that we require $M = 3$ to satisfy the third-order differentiability constraint in Eqs. (7).

To solve for the pseudocontrol spline coefficients, we develop a system of linear equations in each dimension (x,y,h) determined by the partial derivative of the cost function in Eq. (4) with respect to the spline coefficients, and the constraint equations (5-7). The composition of the system of equations for a quadratic spline ($M = 2$) in one dimension is given by

1) N intercept point constraints
2) $N - 1$ continuous acceleration constraints
3) 1 endpoint velocity constraint
4) 1 initial acceleration constraint
5) $3N$ optimization equations

for a total of $5N + 1$ equations. For a cubic spline ($M = 3$),

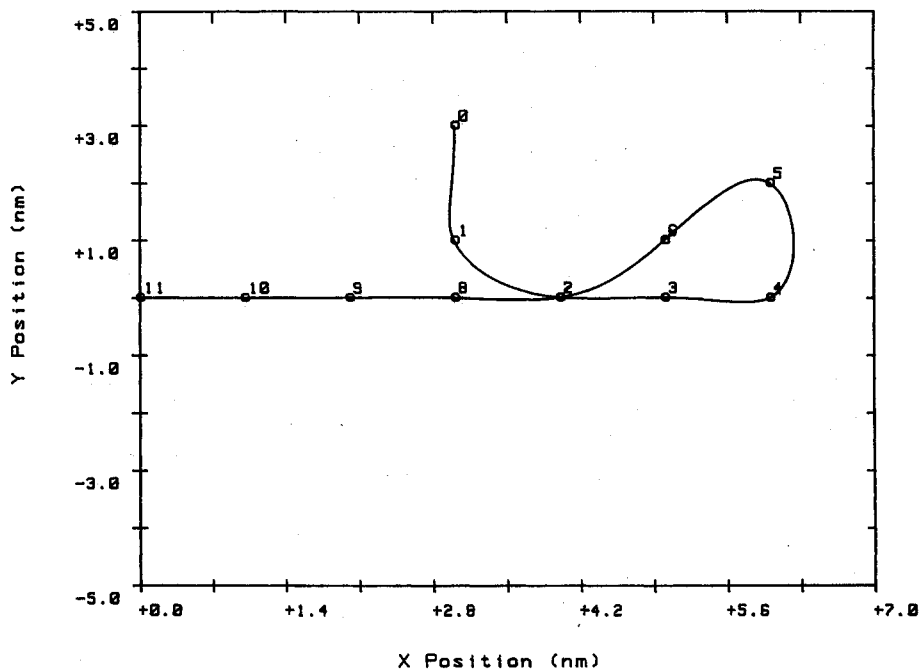

Fig. 2a Dynamic quadratic spline X vs Y position.

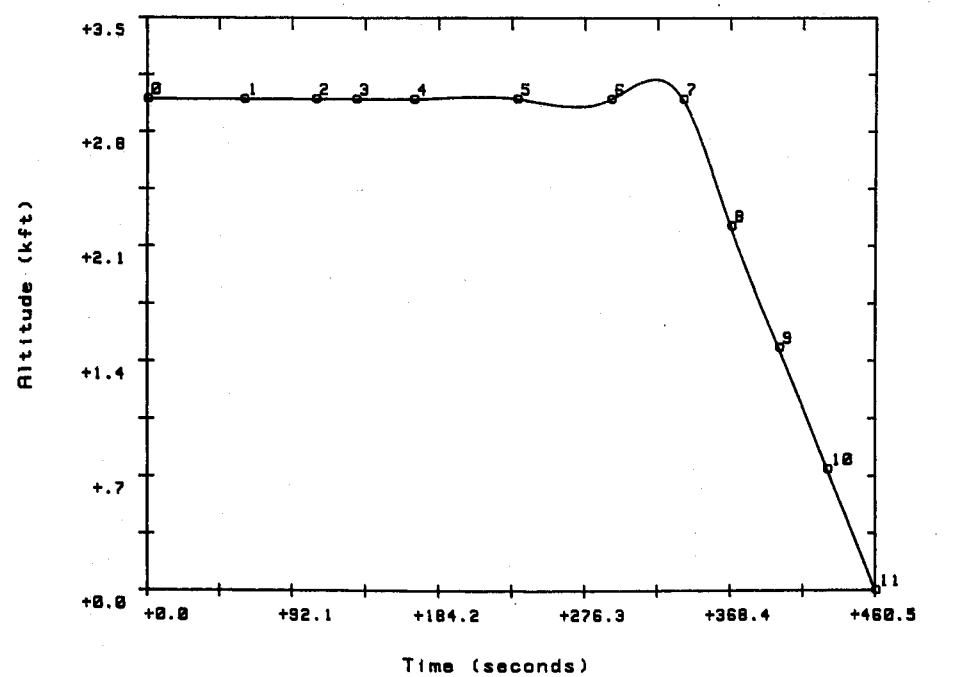

Fig. 2b Dynamic quadratic spline altitude vs time.

$7N$ equations are required per dimension, giving an additional $N-1$ continuous jerk constraints and N optimization equations for the added spline coefficient. Note that the initial position and velocity constraints are not considered in determining the number of spline coefficient equations to solve, since they are simply the initial conditions for Eqs. (3) on the first interval.

These systems of equations were constructed using the waypoints listed in Table 1 for a quadratic spline representation of the pseudocontrols in Eqs. (8). To apply this optimization, the intercept times for the waypoints had to be derived. This was accomplished by first choosing the total velocity of the trajectory as 200 ft/s, so that the initial and final velocities stated in Eqs. (6) are

$$\dot{x}_0 = -200 \text{ ft/s}, \qquad \dot{x}_N = -198.5 \text{ ft/s} \tag{9a}$$

$$\dot{y}_0 = 0, \qquad \dot{y}_N = 0 \tag{9b}$$

$$\dot{h}_0 = 0, \qquad \dot{h}_N = -24.4 \text{ ft/s} \tag{9c}$$

The intercept times can then be computed by dividing the arclength of each interval for the "static" trajectory by the desired velocity of 200 ft/s, and adding the result to the previous waypoint time. These data are tabulated in Table 2, along with the resulting arclength of the static trajectory. The "dynamic" trajectory generated from the solution of the linear equations for the pseudocontrol spline coefficients given the intercept times shown in Table 2, the velocity constraints in Eqs. (9), and zero initial acceleration is shown in Figs. 2a and 2b. The latter constraint was chosen to allow a straight-line intercept to the generated trajectory and maintain continuous acceleration at the initial waypoint. Arclengths for each interval of the dynamic trajectory are listed in Table 2. Observe that the dynamic trajectory differs substantially from the static path (compare Figs. 1a and 1b with 2a and 2b). The most notable discrepancy is that the former curve exhibits larger altitude excursions on intervals 6 and 7 than the latter due to the dynamics introduced by Eqs. (3). These deviations are partially reflected in the interval arclength differences of the two curves (Table 2).

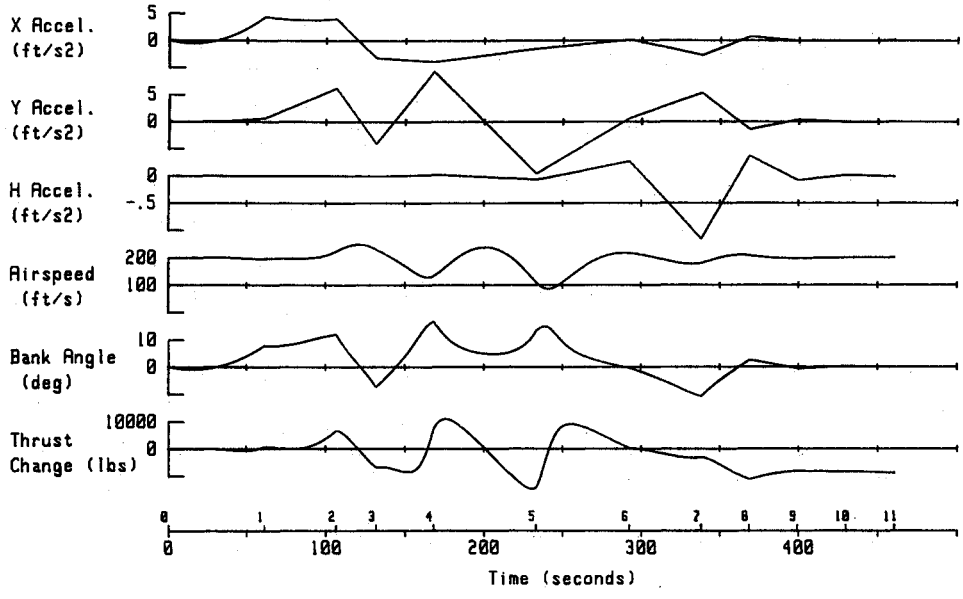

Fig. 2c Dynamic quadratic spline controls vs time.

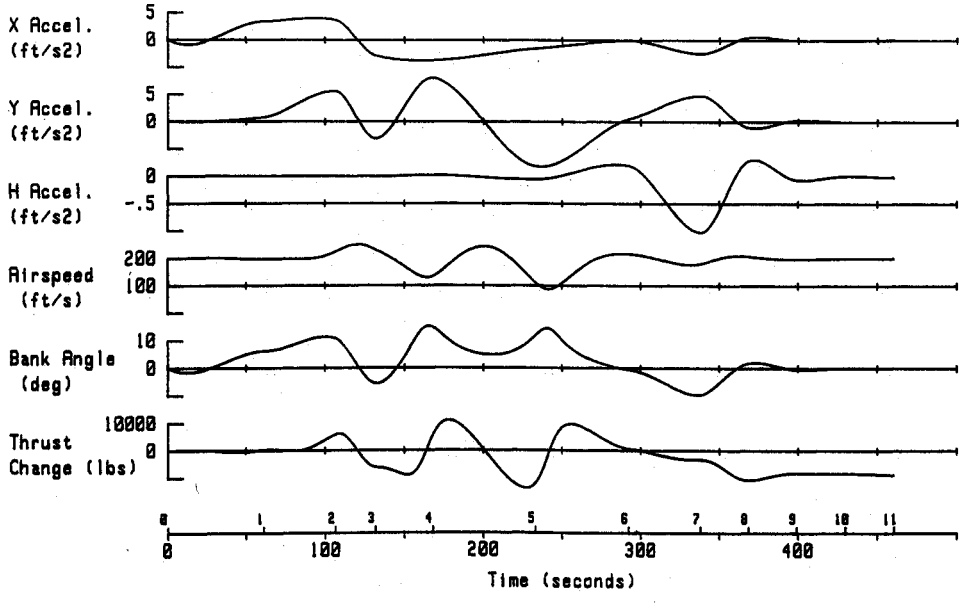

Fig. 2d Dynamic cubic spline controls.

The aircraft accelerations (pseudocontrols), airspeed, bank angle, and thrust as defined in Ref. 11 required for the system of Eqs. (3) to follow the dynamic trajectory are given in Fig. 2c (assumes constant drag). Note the large airspeed excursions off the desired 200-ft/s value, and the thrust changes required for the maneuver. Also notice that the accelerations and controls are not differentiable, which implies an uncomfortable ride to the passengers on board. To improve ride comfort, a cubic spline was applied to the pseudocontrols. Qualitatively, there is no difference in the trajectories generated by either the quadratic or cubic spline pseudocontrols, as evidenced by the minor differences in interval arclengths (Table 2). However, as can be seen in Fig. 2d, the cubic spline affords improved smoothness of controls and accelerations, a desirable feature in any practical application of dynamic interpolation.

To make the dynamic trajectories invariant under affine changes of coordinates in the waypoint data, we can employ affine invariant cost functionals as in the CAGD literature.[9,10] For example, we can modify the cost functional of Eq. (4) as

$$J' = \int_{t_0}^{t_N} Y_m' \, Q(P) \, Y_m \, dt \tag{10}$$

$$Y_m = [\ddot{x}(t), \ddot{y}(t), \ddot{h}(t)]' \tag{11}$$

where $Q(P)$ is defined as

$$Q(P) = [P_0 - \bar{P} | \ldots | P_N - \bar{P}] W [P_0 - \bar{P} | \ldots | P_N - \bar{P}]^{-1}$$

$$0 \le i \le N \tag{12}$$

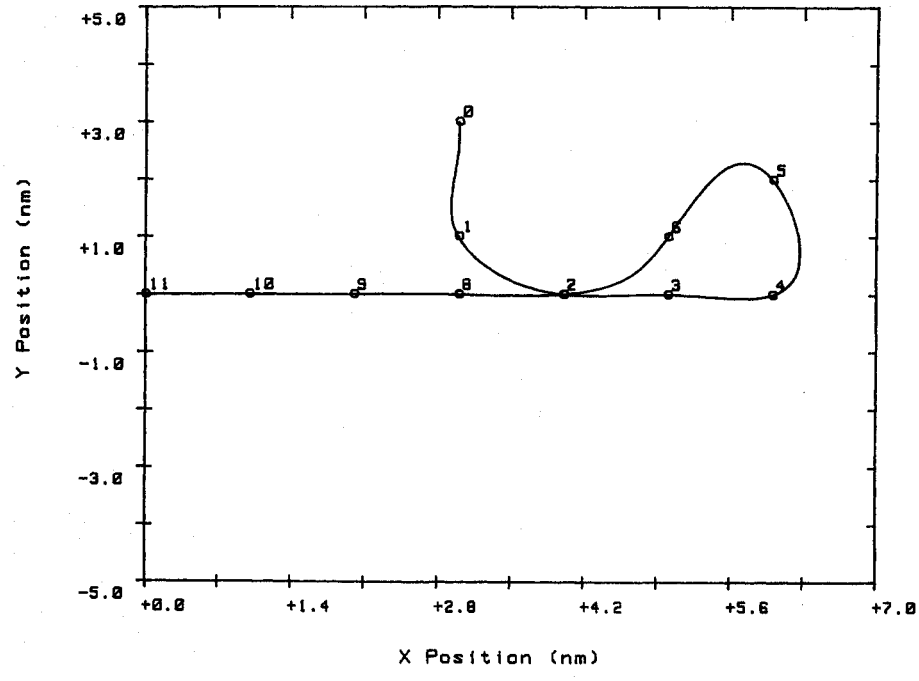

Fig. 3a Arclength iteration X vs Y position.

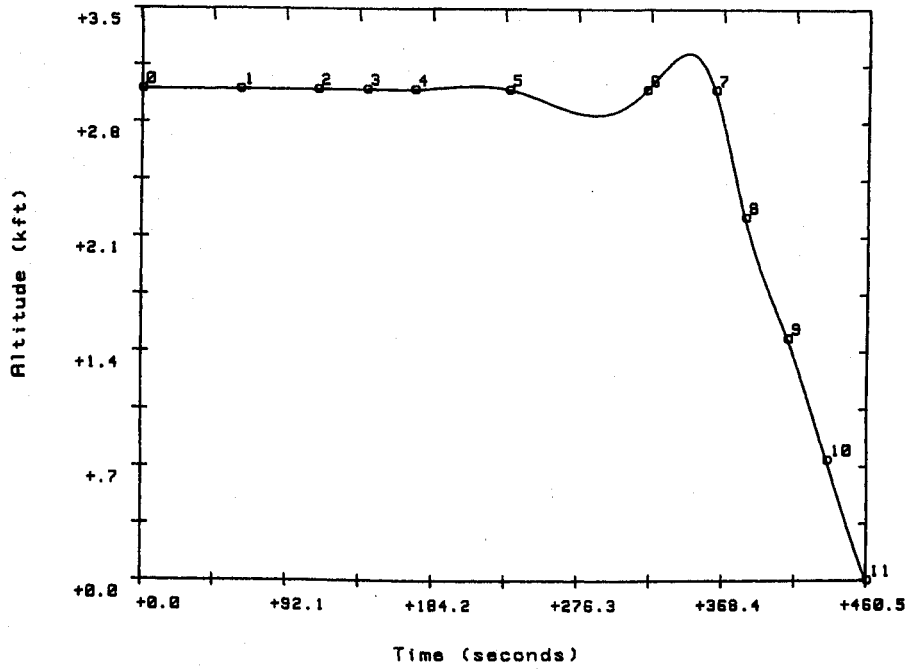

Fig. 3b Arclength iteration altitude vs time.

where

$$P_i = (x_i, y_i, h_i)'$$

$$\bar{P} = \sum_{i=0}^{N} P_i \Big/ (N+1)$$

and W is any positive-definite matrix. Without the use of such a weighted optimization scheme, the trajectories resulting from rescaling the waypoints could lead to vastly different curves, a classical observation in the case of static trajectories.[10]

In summary, the static trajectory derived from CAGD methods was used to derive intercept times for the waypoints required in the dynamic trajectory generation, and to provide a "best-case" reference path for comparing the dynamic results. The application of splines to the pseudocontrols (U_x, U_y, U_h) resulted in a nearly reasonable dynamic trajectory for a difficult approach case. Methods to improve these results will be addressed next.

IV. Improvements in Dynamic Interpolation Results

Given the simple double integrator plant of Eqs. (3) of the aircraft control problem, we consider modifying the intercept times to obtain better dynamic trajectories. These parameters were selected because of the faulty assumption of constant velocity in their derivation, as seen in Figs. 2c and 2d. One measure of a good trajectory generated dynamically would be the "closeness" to the statically generated path, which we consider a best case. This contention is based on the flexibility that CAGD methods afford in generating the static trajectory. We have considered a measure of closeness to be the arclength

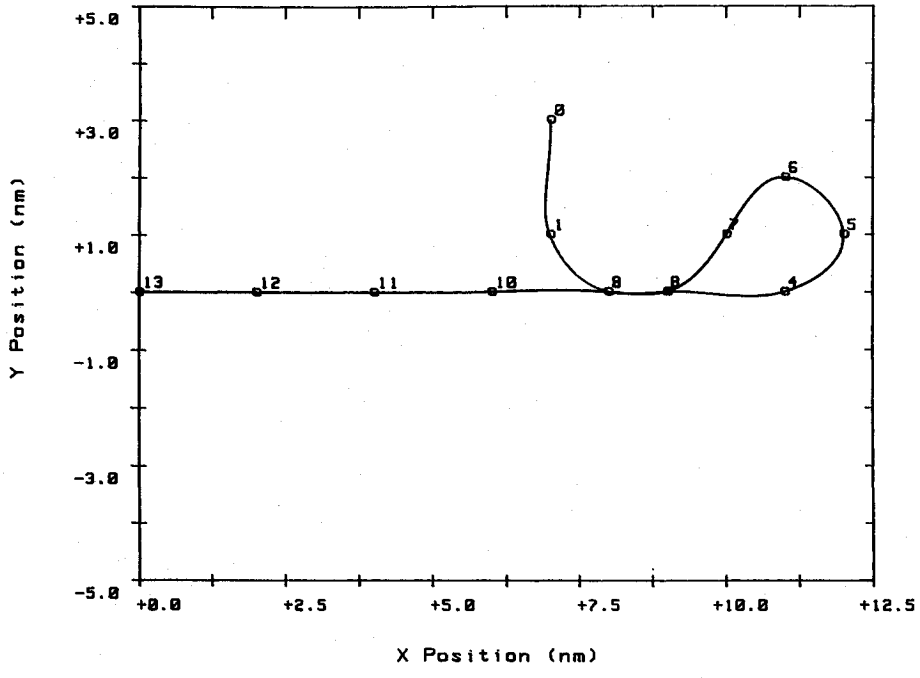

Fig. 4a Commercial aircraft approach X vs Y position.

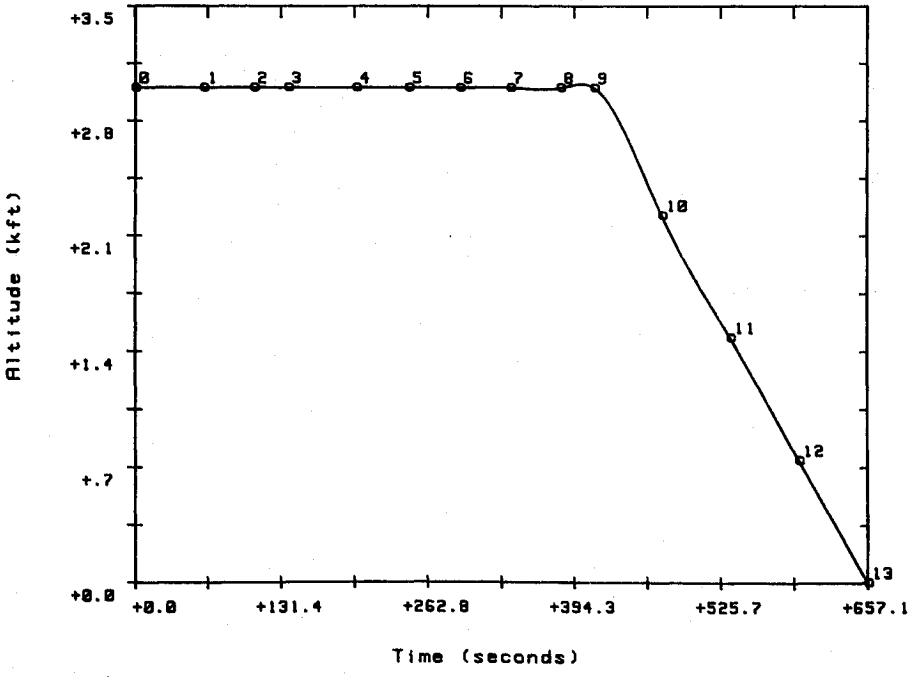

Fig. 4b Commercial aircraft approach altitude vs time.

differences of the two trajectories at each interval. In an attempt to improve the intercept times, we employed approximate Newton-type algorithms in the following manner in which we assume that it is possible for the dynamically generated trajectory to achieve the interval arclengths of the reference trajectory:

$$T^{k+1} = T^k + [F^k]^{-1}(S_d - S^k) \tag{13a}$$

$$T = [t_1, t_2, \ldots, t_{N-1}] = \text{updated intercept time vector} \tag{13b}$$

$$t_N = \text{const (fixed final time)} \tag{13c}$$

$$S_d = [S_{d1}, S_{d2}, \ldots, S_{dN}]' = \text{desired arclength vector} \tag{13d}$$

$$S^k = [S_1^k, S_2^k, \ldots, S_N^k]' = \text{actual arclength vector} \tag{13e}$$

$$S_i^k = \int_{t_{i-1}}^{t_i} [\dot{x}(t)^2 + \dot{y}(t)^2 + \dot{h}(t)^2]^{1/2}\, dt, \qquad 1 \le i \le N \tag{13f}$$

$$F^k = \frac{dS^k}{dT^k} = \text{Jacobian of arclength vector} \tag{13g}$$

Various approximations to the Jacobian matrix $dS^k(T^k)/dT^k \approx F^k$ were employed by ignoring various dependencies of S on T. The final time t_N was assumed fixed so that the average velocity may be kept near 200 ft/s. Iterative application of Eqs. (13) to the cubic spline dynamic trajectory problem of Sec. III results in the intercept times and interval arclengths given in Table 3 and the trajectory shown in Fig. 3. Based on the data in Table 3, the arclength iteration method improved the match between the static and dynamic trajectory interval arclengths. However, application of this method also increased the altitude excursions between waypoints 5 and 7, as can be seen by comparing Figs. 2b and 3b. These results clearly demonstrate that the system dynamics in Eqs. (3) interferes with the ability of the dynamic system to follow a static trajectory exactly, given the simple description of cubic splines for the pseudocontrols.

Recognizing this fact, an alternative procedure was employed that updated the times t_i to minimize the total cost:

$$J = \sum_{i=1}^{N} \int_{t_{i-1}}^{t_i} [U_x^2 + U_y^2 + U_h^2]\, dt \tag{14}$$

In this case, the Jacobian in the Newton algorithm can be evaluated exactly. The intercept times and initial and final costs resulting from the application of the minimum cost algorithm to the static CAGD initial times are tabulated in Table 4. These results indicate that although one can improve the cost criteria by application of the Newton algorithm, the enhancement is slight, demonstrating the difficulty in improving the results obtained using the intercept times generated from the static CAGD result.

Table 3 Arclength iteration results

Interval	Static arclength, ft	Final intercept time, s	Initial dynamic arclength, ft	Final dynamic arclength, ft
1	12,240	62.2	12,210	12,218
2	9,068	111.2	9,124	9,027
3	6,115	142.0	6,089	6,094
4	6,170	172.1	6,242	6,168
5	13,008	231.9	12,736	12,881
6	11,886	319.1	9,460	11,836
7	9,103	362.7	8,818	9,167
8	6,130	382.5	6,163	6,142
9	6,125	409.7	6,126	6,127
10	6,125	434.8	6,126	6,125
11	6,125	460.5	6,127	6,127

Table 4 Minimum cost iteration result

Interval	Initial cost	Final cost	Final intercept time, s
1	193	144	60.5
2	1277	1259	109.1
3	387	340	133.7
4	1287	1248	166.7
5	2439	2590	232.8
6	1749	1691	292.3
7	616	574	339.1
8	315	295	370.3
9	22	16	399.5
10	2	11	428.9
11	1	12	460.5
Total	8288	8180	

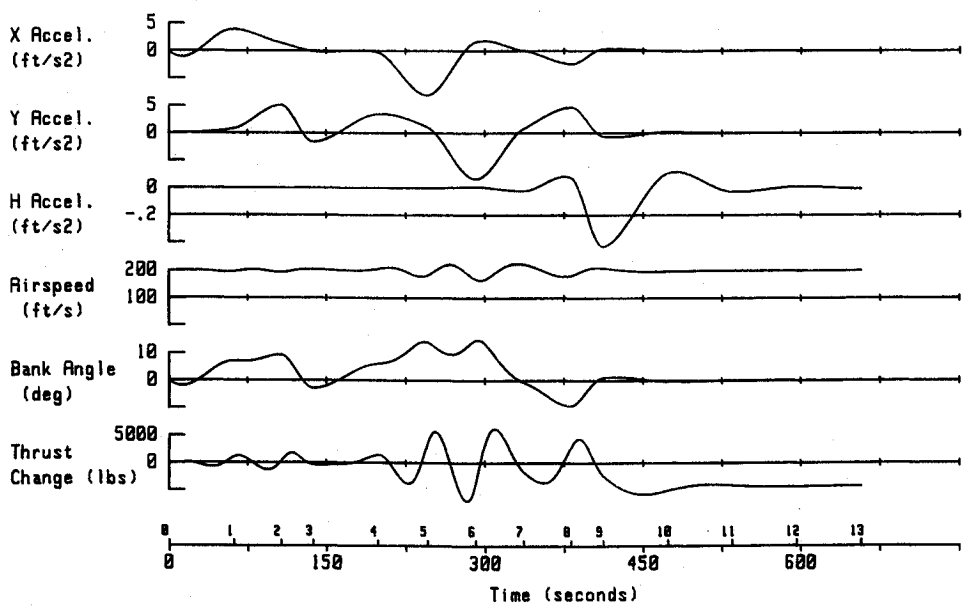

Fig. 4c Commercial aircraft approach controls vs time.

Comparison between the static and dynamic trajectories clearly demonstrates the influence of the system dynamics on the interpolation problem. Indeed, the results of applying the static CAGD results directly to the dynamic case seem remarkably good and difficult to improve on. Additional research and testing are clearly necessary to understand the means and criteria with which to optimize the dynamic interpolation procedure, even without the presence of practical constraints on the trajectories, which are naturally of predominant concern in the related works.[4-8]

The excessive speed and thrust requirements in Fig. 2 indicate that today's commercial aircraft would be unable to fly the given trajectory. For instance, even a low-speed turboprop aircraft such as a DeHavilland DCH8-100, which normally performs approaches near 90 knots (150 ft/s), would likely stall on this approach. Furthermore, the DCH8-100 engines are not rated for the ± 10,000-lb-thrust requirements of the trajectory. Figure 4 gives simulations for a more reasonable teardrop approach whose speed and thrust requirements are more typical of the performance of this type of aircraft. The simulations were generated using cubic splines and intercept times derived from static CAGD interpolation. The ease with which a flyable trajectory can be generated in this case underlines the severity of the previous approach trajectory.

V. Conclusions

The method of splines has been applied to the control of linearizable dynamical systems such that an affine invariant cost functional (total energy) is minimized subject to discrete path constraints. Computer-aided geometric design methods have been applied to derive a reference trajectory for comparison with the dynamic results, and to determine intercept times for the discrete points that the dynamic trajectory is required to intersect. An acceptable trajectory has been generated by the application of these methods to a difficult aircraft approach problem. Arclength and cost iteration schemes were applied to modify the intercept times and so improve the dynamic trajectory in relation to the reference trajectory. Neither of these methods yielded significant improvement in the dynamic trajectory, demonstrating the difficulty in enhancing the basic dynamic interpolation result. Future work will concentrate on a better understanding of the complex dynamic problem and its relation to the static case.

References

[1]Farin, G., *Curves and Surfaces for Computer Aided Design,* Academic, New York, 1988.

[2]Carnahan, B., *Applied Numerical Methods,* Wiley, New York, 1969.

[3]"DO 198—Minimum Operation Performance Standards for Airborne MLS Area Navigation Equipment," Radio Technical Commission for Aeronautics, Rept. SC-151, March 1988.

[4]Erzberger, H., McLean, J. D., and Barman, J. F., "Fixed-Range Optimal Trajectories for Short Haul Aircraft," NASA TND-8115, Dec. 1975.

[5]Erzberger, H., and Lee, H., "Constrained Optimum Trajectories with Specified Range," *Journal of Guidance, Control, and Dynamics,* Vol. 3, No. 1, 1980, pp. 78–85.

[6]Erzberger, H., and McLean, J. D., "Fuel-Conservative Guidance System for Powered-Lift Aircraft," *Journal of Guidance, Control, and Dynamics,* Vol. 4, No. 3, 1981, pp. 253–261.

[7]Lin, C. S., Chang, P. R., and Luh, J. Y. S., "Formulation and Optimization of Cubic Polynomial Joint Trajectories for Industrial Robots," *IEEE Transactions on Automatic Control,* Vol. AC-28, Dec. 1983, pp. 1066–1074.

[8]Luh, J. Y. S., and Lin, C. S., "Approximate Joint Trajectories for Control of Industrial Robots Along Cartesian Paths," *IEEE Transactions on Systems, Man, and Cybernetics,* Vol. SMC-14, May-June 1984, pp. 444–450.

[9]Nielson, G. M., "Coordinate-Free Scattered Data Interpolation," *Topics in Multivariate Approximation,* edited by C. Chui, L. L. Schumaker, and F. Utreras, Academic, New York, 1987, pp. 175–184.

[10]Foley, T. A., and Nielson, G. M., "Knot Selection for Parametric Spline Interpolation," *Mathematic Aspects of CAGD,* edited by T. Lyche and L. L. Schumaker, Academic, New York, 1989, pp. 210–219.

[11]Menon, P. K. A., "Short-Range Nonlinear Feedback Strategies for Aircraft Pursuit-Evasion," *Journal of Guidance, Control, and Dynamics,* Vol. 12, No. 1, 1989, pp. 27–32.